Monthly Notices of the ROYAL ASTRONOMICAL SOCIETY
MNRAS **461,** 2019–2024 (2016)
Advance Access publication 2016 June 20
doi:10.1093/mnras/stw1479

Spectropolarimetry of the Type IIb SN 2008aq*

H. F. Stevance,[1★] J. R. Maund,[1†] D. Baade,[2] P. Höflich,[3] F. Patat,[2] J. Spyromilio,[2] J. C. Wheeler,[4] A. Clocchiatti,[5] L. Wang,[6] Y. Yang[6] and P. Zelaya[5]

[1] *Department of Physics and Astronomy, University of Sheffield, Hounsfield Rd, Sheffield S3 7RH, UK*
[2] *European Organization for Astronomical Research in the Southern Hemisphere, Karl-Schwarzschild-Str. 2, D-85748 Garching. b. München, Germany*
[3] *Department of Physics, Florida State University, 315 Keen Building, Tallahassee, FL 32306-4350, USA*
[4] *Department of Astronomy, University of Texas at Austin, Austin, TX 78712-1205, USA*
[5] *Departamento de Astronomia y Astrofisica, Pontificia Universidad Catolica Casilla 306, Santiago 22, Chile*
[6] *Department of Physics, Texas A&M University, College Station, TX 77843-4242, USA*

Accepted 2016 June 16. Received 2016 June 16; in original form 2016 April 25

ABSTRACT

We present optical spectroscopy and spectropolarimetry of the Type IIb SN 2008aq 16-d and 27-d post-explosion. The spectrum of SN 2008aq remained dominated by Hα P Cygni profile at both epochs, but showed a significant increase in the strength of the helium features, which is characteristic of the transition undergone by supernovae between Type IIb and Type Ib. Comparison of the spectra of SN 2008aq to other Type IIb SNe (SN 1993J, SN 2011dh, and SN 2008ax) at similar epochs revealed that the helium lines in SN 2008aq are much weaker, suggesting that its progenitor was stripped to a lesser degree. SN 2008aq also showed significant levels of continuum polarization at $p_{\rm cont} = 0.70$ ($\pm$0.22) per cent in the first epoch, increasing to $p_{\rm cont} = 1.21$ ($\pm$0.33) per cent by the second epoch. Moreover, the presence of loops in the $q - u$ planes of Hα and He I in the second epoch suggests a departure from axial symmetry.

Key words: supernovae: general – supernovae:individual:2008aq.

1 INTRODUCTION

Note that we recommend the reader also consult the erratum published for this paper as well as chapter 3 and appendix A of Stevance (2019). When massive stars ($M_{\rm ZAMS} > 8\ {\rm M}_{\odot}$) have exhausted their fuel and die, they give rise to some of the most powerful explosions in the Universe: core-collapse supernovae (CCSNe). CCSNe are divided into a number of sub-classes: Type IIP/L SNe, which show prominent hydrogen lines; Type Ib/c SNe, which result from the explosion of progenitors that have been stripped of their hydrogen, or even helium layers by strong winds or binary interactions (Filippenko 1997); and Type IIb SNe, which, despite representing only a small fraction of CCSNe (∼11 per cent), are an essential transitional class whose members evolve from Type II into Type Ib/c SNe. The progenitors of Type IIb SNe are stripped of nearly all of their hydrogen envelope, retaining less than 0.5 ${\rm M}_{\odot}$ (Smith et al. 2011). As such, Type IIb SNe are sensitive probes of mass-loss processes, particularly binary interactions (e.g. Maund et al. 2004; Fox et al. 2014).

Although we know about the progenitors of CCSNe (see Smartt 2009 for a review), the nature of the explosion mechanism remains a partial mystery. A variety of models have been proposed (for reviews in this field see Janka 2012 and Burrows 2013), whose distinguishing observational features can be the geometries of the resulting ejecta. Spectropolarimetry is a unique tool that allows us to probe the 3D shapes of the ejecta of distant SNe at early times.

Linear polarization of the light emitted by SNe is the result of electron scattering, which is the principal source of opacity at early times (Shapiro & Sutherland 1982). The polarization vector of a scattered photon will be perpendicular to the plane of scattering, defined as the plane containing the incident and scattered ray. Consequently, in a spatially unresolved spherical envelope, the polarization vectors originated from regions located $\pi/2$ away from each other will cancel out, resulting in zero net polarization. A departure from spherical symmetry, however, will result in incomplete cancellation, and a polarization excess (Shapiro & Sutherland 1982; McCall 1984), which can then be detected and used to quantify the shape of the ejecta. The intrinsic polarization associated with the continuum is closely related to the ellipticity of the envelope (Höflich 1991), while the polarization associated with individual spectral lines probes structural asymmetries to smaller scales (Wang & Wheeler 2008).

Virtually all CCSNe show an excess of polarization (Wang & Wheeler 2008), but the extent of that excess varies greatly from one type to another. Generally, Type II SNe show low polarization at early times, but as their envelope expands, and the inner core (beneath the hydrogen envelope) is revealed, the levels of polarization rise significantly (e.g. Leonard et al. 2006). Type Ib/c SNe,

* Based on observations made with ESO Telescopes at the Paranal Observatory, under programme 080.D-0107.

★ E-mail: fstevance1@sheffield.ac.uk
† Royal Society Research Fellow.

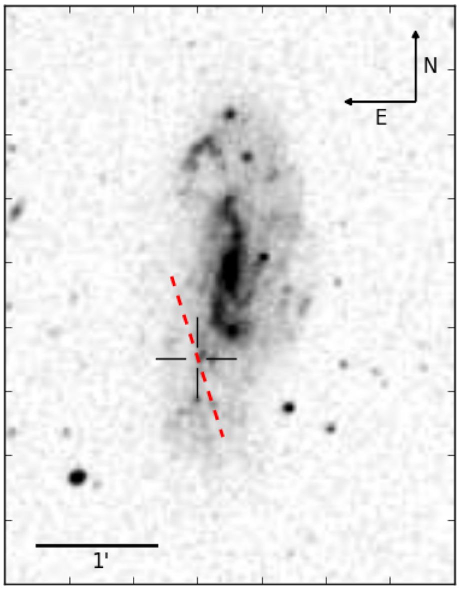

Figure 1. SN 2008aq in MCG-02-33-20. The diagonal line represents the orientation of the ISP (see Section 4.1). This is a Digitized Sky Survey image, retrieved via Aladin.

on the other hand, tend to be significantly polarized at all epochs, and to a higher degree than Type IIP SNe (e.g. Maund et al. 2007a; Maund et al. 2009; Tanaka et al. 2009). Some Type IIb SNe exhibit early polarization levels similar to that of Type IIP/L SNe – e.g. SN 2001ig (Maund et al. 2007c) – but more typical cases such as SN 1993J, SN 1996cb, SN 2008ax, or SN 2011dh show continuum polarization around $p \sim 0.5$ per cent to $p \sim 1$ per cent (Trammell, Hines & Wheeler 1993; Wang et al. 2001; Chornock et al. 2011; Silverman et al. 2009; Mauerhan et al. 2015).

Here, we report spectropolarimetric observations of the Type IIb SN 2008aq. SN 2008aq was discovered by Chu et al. (2008), on 2008 February 27.44, in the galaxy MCG-02-33-20 (see Fig. 1), which has a recessional velocity[1] of 2407 km s^{-1}, and was subsequently classified by Modjaz et al. (2014) as a Type IIb SN. Based on a comparison of the light curve of SN 2008aq published by Bianco et al. (2014) to that of similar Type IIb SNe (SN 1993J and SN 2008ax), we estimate that SN 2008aq was discovered approximately 8 d before *V*-band maximum. The date of the explosion was taken to be 20 d prior to *V*-band maximum, as done by Kumar et al. (2013), following the study of Type IIb and Type Ib/c SNe light curves by Richardson, Branch & Baron (2006). Consequently, we conclude that SN 2008aq exploded on 2008 February 16.

2 OBSERVATIONS AND DATA REDUCTION

Spectropolarimetric observations of SN 2008aq were acquired with Focal Reducer and low dispersion Spectrograph (FORS) on the European Southern Observatory (ESO) Very Large Telescope (VLT), in its dual-beam spectropolarimeter 'PMOS' mode (Appenzeller et al. 1998). Observations of SN 2008aq were conducted at two epochs: 2008 Mar 4.3 and 15.2, a few days before and about a week after *V*-band maximum, respectively. A summary of observations is given in Table 1. Based on our estimate of the explosion date, the observations correspond to ∼16 and 27 d post-explosion.

[1] Found on https://ned.ipac.caltech.edu

Table 1. VLT observations of SN 2008aq.

Object	Date (UT)	Exposure (s)	Epoch (d)	Airmass (avg.)
SN 2008aq	2008 Mar 04.3	4 × 900	+16	1.119
EG274	2008 Mar 04.4	10	+16	1.047
SN 2008aq	2008 Mar 15.2	2 × 4 × 900	+27	1.073
GD108	2008 Mar 15.2	60	+27	1.067

Both sets of observations used the 300*V* grism, providing a spectral resolution of 12.5 Å at 6000 Å (as determined from arc lamp calibration frames). These observations did not use an order separation filter, such that the observations covered a wavelength of 3400–9300 Å at the expense, however, of possible second-order contamination at redder wavelengths. The data were reduced in the standard manner using IRAF[2] following the prescription of Maund et al. (2007b). The Stokes parameters were calculated following the routines of Patat & Romaniello (2006), with the data rebinned to 15 Å to improve levels of signal-to-noise ratio. We investigated the second order contamination effect resulting from not using an order sorting filter by using standard stars that were observed with and without order sorting filters. We find that the second-order effect at 7000 Å (i.e the cut-on wavelength of the grism efficiency) and long-wards are well below the noise level in our data. Flux spectra of SN 2008aq were calibrated against observations of flux standard stars acquired with the polarimetry optics in place.

3 RESULTS

3.1 Optical spectroscopy

The flux spectra of SN 2008aq on 2008 March 4 and 15 are plotted in Fig. 2, along with the flux spectra of SN 1993J, SN 2008ax and SN 2011dh (all Type IIb SNe; obtained from WISeREP[3]; Yaron & Gal-Yam 2012) at similar epochs, for comparison.

At 16 d post-explosion, the spectrum of SN 2008aq is dominated by broad P Cygni profiles of Ca II H&K and Hα; their absorption minima correspond to velocities of $-13\,700$ km s^{-1} and $-12\,000$ km s^{-1}, respectively. The Hα emission appears to be flat topped due to a weak blue-shifted He I λ6678 absorption feature, which is common to the other Type IIb SNe. This feature evolves into a 'notch' at 6530 Å by the second epoch. The velocity at the absorption minimum of Hα was found to be $-11\,700$ km s^{-1} at +27 d. An absorption feature due to He I λ5876 was observed with a velocity of -7800 km s^{-1} and -7350 km s^{-1} in the first and second epochs, respectively. The strength of this feature increases by the second epoch, and a He I λ7065 feature emerges, with a velocity of -7000 km s^{-1}. Additionally, two narrow absorption lines can be seen superposed on to the emission component of He I λ5876, due to Na I D originating in the Milky Way, and at the recessional velocity of the host galaxy. The absorption observed around 8200 Å is attributed to the Ca II Infra-Red (IR) triplet, with a velocity of $-12\,000$ km s^{-1} at 16 d post-explosion. The Ca II IR triplet P

[2] IRAF is distributed by the National Optical Astronomy Observatory, which is operated by the Association of Universities for Research in Astronomy (AURA) under a cooperative agreement with the National Science Foundation.

[3] The Weizmann interactive supernova data repository – http://wiserep.weizmann.ac.il

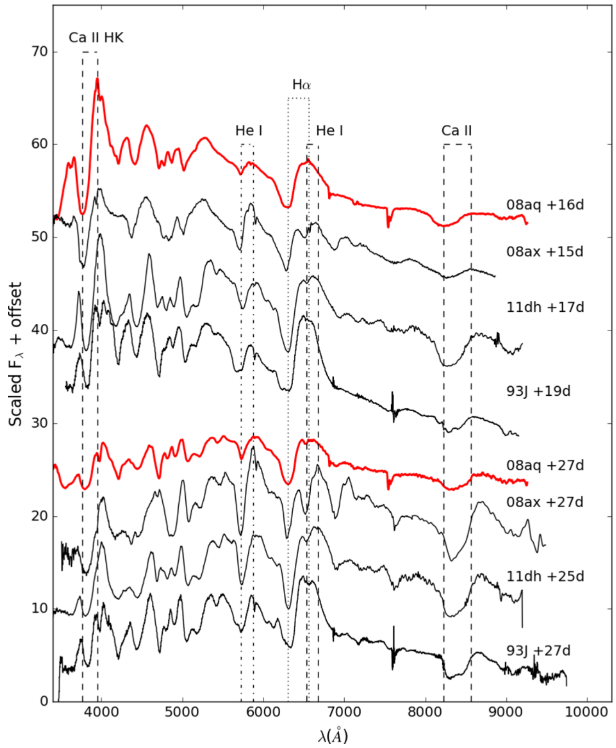

Figure 2. Flux spectra of SN 2008aq (shown in red) at 16 and 27 d post-explosion. Also shown are spectra of SN 1993J, SN 2008ax, and SN 2011dh (in black). For each identified element, two lines were drawn, showing the rest wavelength and the wavelength at absorption minimum. The lines were identified by eye. All of the spectra are corrected for the recessional velocity of their respective host galaxies.

Cygni profile is peculiar in that it exhibits a relatively deep absorption paired with a weak emission component. Branch et al. (2002) noted that this behaviour is characteristic of a 'detached' line forming region at velocities significantly greater than that of the photosphere. By the second epoch, 10 d later, the velocity of the Ca II IR triplet has decreased dramatically to a value of -9000 km s^{-1} and the P Cygni profile shows a prominent emission component. In the second epoch, the velocity of the Ca II IR triplet and Ca H & K features has decreased more noticeably than that of other elements.

The most remarkable difference between SN 2008aq and the comparison SNe (see Fig. 2) is the relative weakness of the He I features. In the first epoch (+16 d) the He I λ5876 line is much shallower in SN 2008aq than in SN 2008ax, SN 1993J or SN 2011dh. Also the presence of a He I λ6678 feature can be inferred from the flat-topped profile of the Hα emission component, whereas in SN 2008ax, SN 2011dh and SN 1993J, this feature is clearly visible in the form of a 'notch'. In the second epoch (27 d post-explosion), the He I lines of SN 2008aq have significantly increased in strength, but are still much weaker than in the spectra of the other Type IIb SNe, and Hα remains the dominant feature. Additionally, the Ca II IR triplet feature at the second epoch is much shallower in the spectrum of SN 2008aq than in the spectra of 1993J, 2011dh and 2008ax, whereas in the first epoch the strength of that feature is similar for SN 2008aq, SN 2008ax and SN 2011dh.

3.2 Spectropolarimetry

The polarization and flux spectra for SN 2008aq are shown in Fig. 3. The median polarization across the spectrum is p ~0.5 per cent in the first epoch, and rises to p ~1 per cent by the second epoch. Significant deviations from these values correlate with the major spectral features. The polarization spectrum at 16 d is

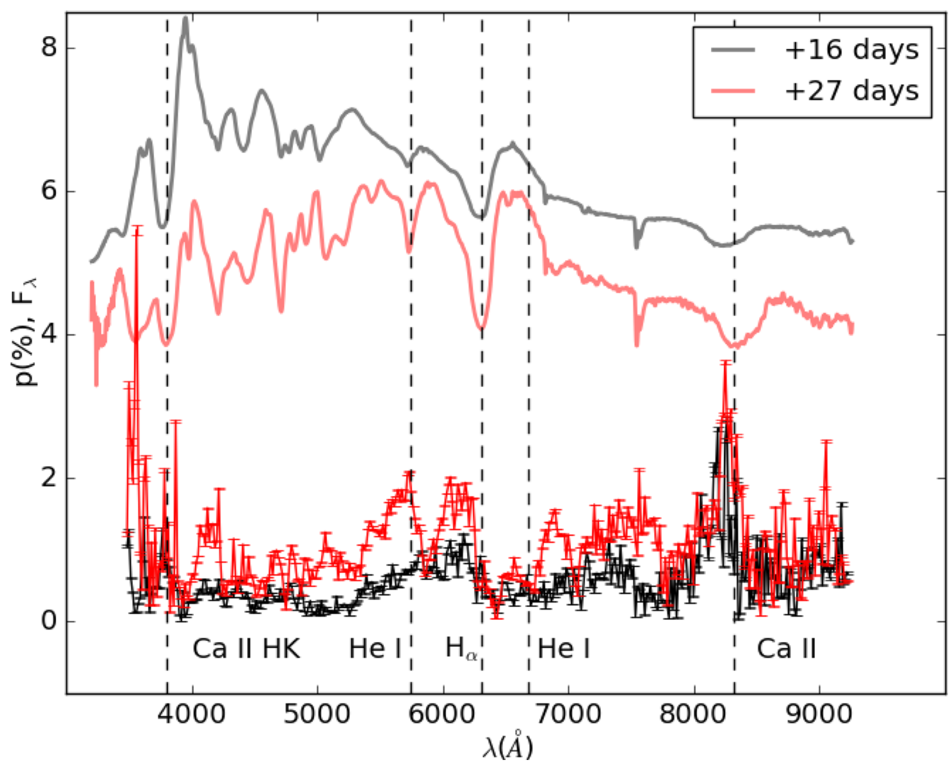

Figure 3. Scaled flux spectra (top) and polarization spectra (bottom) of SN 2008aq at 16 d and 27 d post-explosion. The polarization spectra were not corrected for ISP.

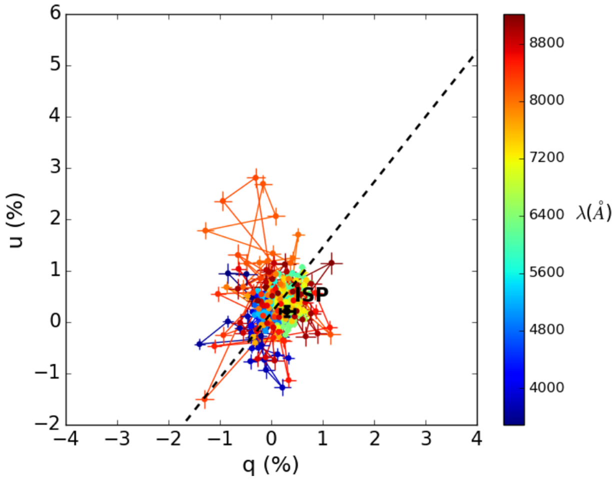

Figure 4. Spectropolarimetric data of SN 2008aq on the 2008-03-04 (16 d after explosion), presented on the Stokes $q - u$ plane. The ISP is marked as a black point, and the dominant axis is represented by the dashed line. The data are colour coded according to wavelength.

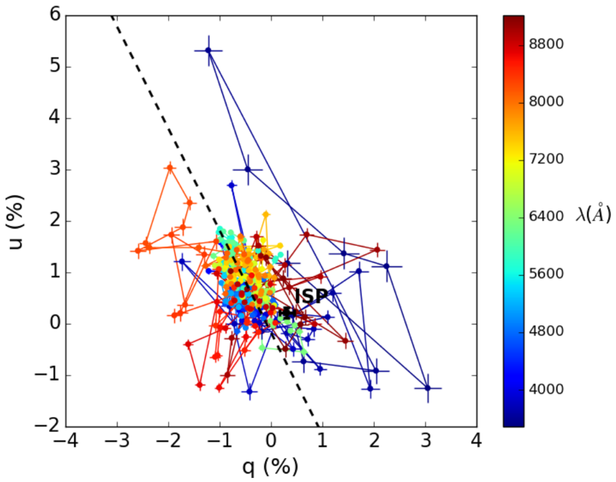

Figure 5. Same figure as Fig. 4, but for the 15th of March 2008, or 27 d after explosion.

dominated by the broad inverse P Cygni profiles of Hα and the Ca II IR triplet, with maximum polarizations of 0.9 ($\pm$0.2) per cent and 1.5 ($\pm$0.6) per cent, respectively. Values of peak polarization were obtained by averaging the data in a range of 250 Å around the centre of the peaks. It should be noted that the red part of the spectrum is contaminated by a high level of noise caused by fringing. At 27 d, the relative strength of the polarization associated with the He I $\lambda\lambda$ 5876, 6678, 7065 features has considerably grown, and the inverse P Cygni profile related to the He I λ5876 line is as prominent as that of Hα. The polarization associated with the Ca II IR triplet has also increased by the second epoch, with a maximum around 2.8 ($\pm$0.4) per cent. Also, depolarization is observed at both epochs between ~4250 and 5300 Å due to line blanketing caused by a blend of iron lines in that region of the spectrum.

The spectropolarimetric data at both epochs are plotted on the Stokes $q - u$ plane in Figs 4 and 5. At both epochs, a dominant axis was fitted to the data using an Orthogonal Distance Regression package in PYTHON.[4] The whole spectrum lies along the respective dominant axes in the form of a tight, elongated cluster of points. The exception is the wavelength range associated with the Ca II IR triplet, which is clearly separate from the dominant axes and the rest of the data in both epochs. Fringing in this wavelength range results in a high level of noise on individual points, but the overall deviation of the Ca II IR triplet is real. A rotation of the dominant axis by ~65 ° is observed between both epochs, which corresponds to a change in PA ~32°.5.

4 ANALYSIS

4.1 Interstellar polarization

The light we receive from the SN may also be polarized by dust in the interstellar medium between us and the object. The interstellar polarization (ISP) component must be quantified to permit proper analysis of the data.

If the assumption of a standard Serkowski-Galactic type ISP is made (Serkowski 1973), the ISP can be constrained using the relationship $p_{\rm ISP} \leq 9 \times E(B-V)_{\rm total}$, where $E(B-V)_{\rm total}$ is the sum of the reddening in the Milky Way and the host galaxy towards SN 2008aq. An empirical relationship relating the equivalent width of the sodium lines and the reddening was derived by Poznanski, Prochaska & Bloom (2012). From the Na I D of the Milky Way component, we estimate that the reddening associated with dust in our Galaxy is $E(B-V)_{\rm MW} = 0.045$ mag, which is in agreement with the estimates of foreground reddening of $E(B-V)_{\rm MW} = 0.04$ mag by Schlafly & Finkbeiner (2011).[5] The reddening associated with the host galaxy was estimated from the corresponding Na I D line, yielding $E(B-V)_{\rm host} = 0.027$ mag. Consequently, the total reddening is $E(B-V)_{\rm total} = 0.072$ mag, which is similar to the value found and used by Stritzinger et al. (2009). The upper limit on the ISP associated with our data is therefore 0.65 per cent.

If we make the assumption that the emission component of Hα is intrinsically unpolarized at early times (Tran et al. 1997), then the average polarization over that feature must be due solely to the ISP – for a discussion on the veracity of this assumption, see Section 5. Therefore, we averaged the values of the Stokes parameters in the range 6700–6900 Å to determine more precise values of the ISP, and found $q_{\rm ISP} = 0.31$ ($\pm$0.14) and $u_{\rm ISP} = 0.22$ ($\pm$0.10), corresponding to $p_{\rm ISP}$ ~0.38 per cent. These values were subsequently used for the correction of the ISP.

4.2 Continuum polarization

After correction for the ISP, the polarization level of the continuum was calculated by averaging the values of p in the range 7000–7500 Å. We assumed the range 7000–7500 Å was representative of the continuum due to the absence of any strong lines in the flux spectrum. The corresponding uncertainty was taken to be the standard deviation of the polarization over this range. Values of $p_{\rm cont}$= 0.70 ($\pm$0.22) per cent and $p_{\rm cont}$ = 1.21 ($\pm$0.33) per cent were measured at +16 d and +27 d, respectively. The polarization of the continuum is an indication of the overall geometry of the envelope. Höflich (1991) performed Monte Carlo calculations for axisymmetric scattering dominated atmospheres, and his fig. 4 shows the relation between the continuum polarization and the axis ratio of the

[4] http://docs.scipy.org/doc/scipy/reference/odr.html
[5] https://ned.ipac.caltech.edu/

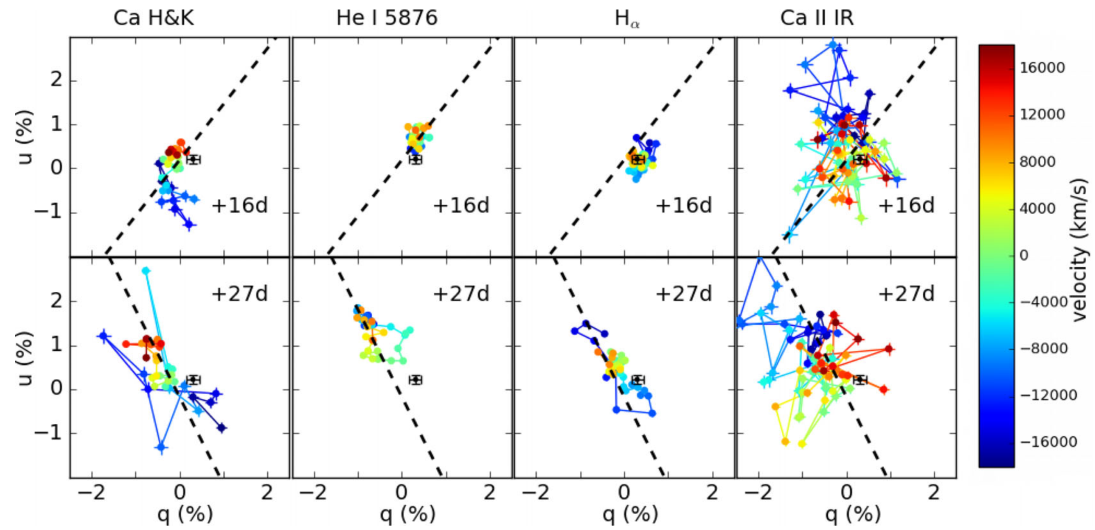

Figure 6. Spectropolarimetric data associated with the absorption components of the P Cygni profiles of Ca H&K, Hα, He I λ5876 and the Ca II IR triplet at +16 d (top panels) and +27 d (bottom panels). The colour scheme illustrates their velocity with respect to rest wavelength. The black point represents the ISP, and the dashed lines represent the same dominant axes as in Figs 4 and 5.

envelope. Comparing our values of the continuum polarization to Höflich (1991), the axis ratios at the first and the second epoch were ∼0.8–0.9, under the assumption that the continuum polarization is solely due to the geometry of the ejecta.

The polarization angle of the continuum was evaluated in the same wavelength range as $p_{\rm cont}$, and found to be 55° (±44°) in the first epoch, and 67°(±20°) in the second epoch. Within the given uncertainties, it is unclear if the continuum polarization angle remained fixed between 16 d and 27 d post-explosion, or underwent a change similar to the rotation of the dominant axis (∼32.°5; see Section 3.2).

4.3 Line polarization

The polarization measured across Ca H& K, He I λ5876, Hα and the Ca II IR triplet is presented in the form of $q - u$ plots (see Fig. 6).

At +16 d, He I λ5876 and Hα show low intrinsic polarization levels (i.e. q and u close to 0), and the data are clustered close to the dominant axis. By + 27 d, clear loops arise, both in He I λ5876 and Hα, which follow the direction of the dominant axis. Loops on the $q - u$ plane indicate that the degree of polarization changes with velocity, and hence with depth, suggesting departure from axi-symmetry on a small scale. The superposition of loops from line polarization along a common direction, however, is principally responsible for the dominant axes as they appear in Figs 4 and 5. The rotation of the dominant axes between the two epochs implies a real rotation in the axial symmetry of the ejecta (in particular line forming region), even though a change in the continuum polarization is inconclusive (see Section 4.2).

The data associated with Ca H& K 16 d post-explosion also show a loop, but it is not oriented in the direction of the dominant axis, which could suggest a significant departure from axial symmetry. At +27 d, the data show substantial scatter, which is most likely the result of the high level of noise in this region of the spectrum, therefore making definite conclusions challenging to draw. The Ca II IR triplet data approximately follow the dominant axes at both epochs, but the signal is also very noisy and it is not possible to confidently ascertain the presence of loops.

5 DISCUSSION AND CONCLUSION

Optical spectra and spectropolarimetric data of SN 2008aq were presented at two epochs: 16 d and 27 d post-explosion. The intrinsic polarization calculated for SN 2008aq at +16 d ($p_{\rm cont}$ = 0.70 ±0.22 per cent) is similar to that of SN 2008ax at +9 d ($p_{\rm cont}$ = 0.64 ±0.02 per cent) and SN 2011dh at +14 d ($p_{\rm cont}$ ∼0.5 per cent) (Chornock et al. 2011; Mauerhan et al. 2015). By the second epoch, the continuum polarization of SN 2008aq had reached a value of $p_{\rm cont}$ = 1.21 (±0.33) per cent, which is close to the continuum polarization calculated for SN 1993J at +29 d ($p_{\rm cont}$ ∼1 per cent) by Tran et al. (1997).

A characteristic of Type IIb SNe is the increase in strength of their He features with time, as they transition to Type Ib SNe. This behaviour is observed in SN 2008aq (see Section 3.1), however, comparison with other Type IIb SNe at similar epochs reveals that the He features in the spectra of SN 2008aq are significantly weaker (see Fig. 2). Additionally, we found that the pseudo-equivalent width of the He I λ5876 absorption component at both epochs was roughly four to five times smaller in SN 2008aq than in other Type IIb SNe (Liu et al. 2015). The scarcity of helium indicates that the receding photosphere of SN 2008aq reached the helium layer at a later date than in SN2008ax, SN 2011dh, SN 1993J, and other previously studied Type IIb SNe; this may suggest that the progenitor of SN 2008aq was stripped of hydrogen to a lesser extent than other Type IIb SNe.

Like other Type IIb SNe, e.g. SN 1993J (Tran et al. 1997) and SN 2001ig (Maund et al. 2007c), SN 2008aq showed a drastic dominant axis rotation between +16 and +27 d (see Figs 4 and 5), suggesting a change in the axis of symmetry deeper into the envelope. Additionally, as we have seen in Section 4.3, loops arise in the $q - u$ planes of Hα and He I λ5876 by +27 d, indicating departures from axial symmetry in the Hα and He I line forming regions (Wang & Wheeler 2008). Therefore, both the overall geometry and smaller scale geometry of the envelope of SN 2008aq vary with depth. Additionally, the polarization of the Ca II IR triplet is greater than that of Hα and He I at both epochs. Also considering the dramatic decrease in velocity of Ca II between the two epochs, compared to Hα and He I, it can be concluded that the line forming region of Ca II and the line forming region of Hα and He I are separate.

Our determination of the ISP is dependent on the assumption that the Halpha P Cygni profile at early times is completely depolarized (e.g. Trammell et al. 1993; Tran et al. 1997); however, the emission component of Hα at +16 d is flat-topped which, as mentioned in Section 3, is indicative of the presence of a He I λ6678 feature. Hence, the polarization associated with this part of the Hα P Cygni profile might be contaminated by polarization associated with He I λ6678. If, as we have shown in Maund et al. (2007c), contamination by the He I 6678 feature masks intrinsic polarization then our determination of the ISP is likely to be an underestimate. Since this work studies the variations of the polarization across the lines, the absolute value of the derived polarization is of interest but not critical to our conclusions. It is also worth noting that the ISP has a wavelength dependence (Serkowski 1973). The ISP we derive, however, is small and therefore the wavelength dependence is likely to be negligible for our results.

ACKNOWLEDGEMENTS

The authors would like to thank ESO for the generous allocation of observing time, as well as the staff of the Paranal Observatory for their work on the program 080.D-0107. FS is supported through a PhD scholarship granted by the University of Sheffield. The research of JRM is supported through a Royal Society University Research Fellowship. JCW is supported by NSF Grant AST 11-09881. This research has made use of the NASA/IPAC Extragalactic Database (NED) which is operated by the Jet Propulsion Laboratory, California Institute of Technology, under contract with the National Aeronautics and Space Administration.

REFERENCES

Appenzeller I. et al., 1998, The Messenger, 94, 1
Bianco F. B. et al., 2014, ApJS, 213, 19
Branch D. et al., 2002, ApJ, 566, 1005
Burrows A., 2013, Rev. Modern Phys., 85, 245
Chornock R. et al., 2011, ApJ, 739, 41
Chu J., Li W., Filippenko A. V., Blondin S., Narayan G., 2008, Central Bureau Electronic Telegrams, 1271
Filippenko A. V., 1997, ARA&A, 35, 309
Fox O. D. et al., 2014, ApJ, 790, 17
Höflich P., 1991, A&A, 246, 481
Janka H.-T., 2012, Annu. Rev. Nucl. Part. Sci., 62, 407
Kumar B. et al., 2013, MNRAS, 431, 308
Leonard D. C. et al., 2006, Nature, 440, 505
Liu Y.-Q., Modjaz M., Bianco F. B., Graur O., 2015, preprint (arXiv e-prints)
McCall M. L., 1984, MNRAS, 210, 829
Mauerhan J. C. et al., 2015, MNRAS, 453, 4467
Maund J. R., Smartt S. J., Kudritzki R. P., Podsiadlowski P., Gilmore G. F., 2004, Nature, 427, 129
Maund J. R., Wheeler J. C., Patat F., Baade D., Wang L., Höflich P., 2007a, A&A, 475, L1
Maund J. R., Wheeler J. C., Patat F., Baade D., Wang L., Höflich P., 2007b, MNRAS, 381, 201
Maund J. R., Wheeler J. C., Patat F., Wang L., Baade D., Höflich P. A., 2007c, ApJ, 671, 1944
Maund J. R., Wheeler J. C., Baade D., Patat F., Höflich P., Wang L., Clocchiatti A., 2009, ApJ, 705, 1139
Modjaz M. et al., 2014, AJ, 147, 99
Patat F., Romaniello M., 2006, PASP, 118, 146
Poznanski D., Prochaska J. X., Bloom J. S., 2012, MNRAS, 426, 1465
Richardson D., Branch D., Baron E., 2006, AJ, 131, 2233
Schlafly E. F., Finkbeiner D. P., 2011, ApJ, 737, 103
Serkowski K., 1973, in Greenberg J. M., van de Hulst H. C., eds, Interstellar Dust and Related Topics Vol. 52 of IAU Symposium, Interstellar Polarization (review). IAU, p. 145
Shapiro P. R., Sutherland P. G., 1982, ApJ, 263, 902
Silverman J. M., Mazzali P., Chornock R., Filippenko A. V., Clocchiatti A., Phillips M. M., Ganeshalingam M., Foley R. J., 2009, PASP, 121, 689
Smartt S. J., 2009, ARA&A, 47, 63
Smith N., Li W., Filippenko A. V., Chornock R., 2011, MNRAS, 412, 1522
Stevance H. F., 2019, preprint (arXiv:1906.07184)
Stritzinger M. et al., 2009, ApJ, 696, 713
Tanaka M. et al., 2009, ApJ, 699, 1119
Trammell S. R., Hines D. C., Wheeler J. C., 1993, ApJ, 414, L21
Tran H. D., Filippenko A. V., Schmidt G. D., Bjorkman K. S., Jannuzi B. T., Smith P. S., 1997, PASP, 109, 489
Wang L., Wheeler J. C., 2008, ARA&A, 46, 433
Wang L., Howell D. A., Höflich P., Wheeler J. C., 2001, ApJ, 550, 1030
Yaron O., Gal-Yam A., 2012, PASP, 124, 668

This paper has been typeset from a TEX/LATEX file prepared by the author.